

The Phase Diagram of QCD

Simon Hands

*Department of Physics, University of Wales Swansea,
Singleton Park, Swansea SA2 8PP, U.K.*

Abstract: I use simple thermodynamic reasoning to argue that at temperatures of order a trillion kelvin, QCD, the theory which describes strongly interacting particles such as protons and neutrons under normal conditions, undergoes a phase transition to a plasma of more elementary constituents called quarks and gluons. I review what is known about the plasma phase both from theoretical calculations and from experiments involving the collisions of large atomic nuclei moving at relativistic speeds. Finally I consider the behaviour of nuclear material under conditions of extreme density, and discuss possible exotic phenomena such as quark matter and color superconductivity.

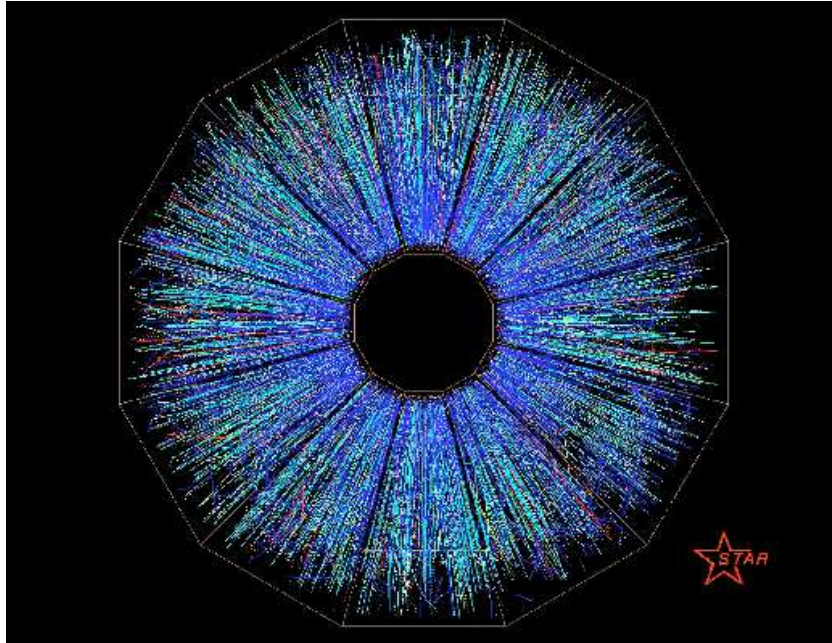


Figure 1: Au+Au collision in the STAR detector at the Relativistic Heavy Ion Collider
(courtesy Brookhaven National Laboratory)

1 Introduction

For over 25 years, our best theory of the strong interaction responsible for binding together protons and neutrons within the atomic nucleus has been Quantum Chromodynamics, or QCD for short. QCD treats nucleons not as fundamental objects in their own right, but as composite states of size roughly 1fm ¹ made from more elementary particles called *quarks*. Quarks have spin- $\frac{1}{2}$ and come in several varieties, or *flavors*; the two lightest quarks are the up quark u , which carries an electric charge $+\frac{2}{3}e$, where e is the absolute value of the electron charge, and the down quark d which has charge $-\frac{1}{3}e$. Table 1 summarises the important properties of the known quarks. Note that we specify both “constituent” and “current” quark masses, a distinction to be explained below. Constituent and current masses can differ considerably for the lighter flavors u, d, s – the origin of the $O(10^4)$ factor between heaviest and lightest current masses is as yet not understood. With an eye to the charge and constituent mass assignments of Table 1, we can identify a proton as a uud bound state with net charge $+e$ and the neutron as udd with net charge zero.

Table 1: Summary of properties of the known quarks

quark flavor	symbol	charge Q/e	constituent mass Σ (MeV/ c^2)	current mass m (MeV/ c^2)
down	d	$-\frac{1}{3}$	~ 350	~ 7
up	u	$+\frac{2}{3}$	~ 350	~ 3
strange	s	$-\frac{1}{3}$	~ 550	~ 140
charm	c	$+\frac{2}{3}$	~ 1800	~ 1800
bottom	b	$-\frac{1}{3}$	$\sim 4.2 \times 10^3$	$\sim 4.2 \times 10^3$
top	t	$+\frac{2}{3}$	$\sim 170 \times 10^3$	$\sim 170 \times 10^3$

The experimental support for this picture is two-fold. Firstly, the quark model provides a very natural explanation for the multiplicity and pattern of strongly-interacting particles (collectively known as *hadrons*) briefly formed in high-energy particle collisions [1]. Hadrons can be classified as either three-quark qqq states called *baryons*, such as nucleons, or quark – anti-quark $q\bar{q}$ states called *mesons*, the lightest example being the pi-meson or pion, which occurs in three charge states π^\pm and π^0 , all with roughly one-seventh the mass of the proton. Apart from nucleons and pions, most hadrons decay via the strong interaction and have typical lifetimes of $O(10^{-23}\text{s})$. Their variety can be accounted for by differing combinations of quark spin and flavor,

¹fm stands for *femtometre*, also known as a *fermi*. $1\text{fm} = 10^{-15}\text{m}$.

as well as various radial excitation states. Secondly, the results of high energy inelastic scattering experiments of electrons off nucleons are consistent with the presence of pointlike spin- $\frac{1}{2}$ constituents called *partons*, just as high-angle Rutherford scattering of α -particles off atoms demonstrates the existence of the nucleus. The partons appear to be able to move freely within the nucleon volume [2], and it is natural to identify them with quarks. In still higher energy e^+e^- experiments rather well-collimated sprays or *jets* of particles, all with similar momenta, emerge from the event region. These are most naturally explained by a single progenitor quark scattered in the original high-energy collision, which subsequently decays into a profusion of lower energy hadrons. Paradoxically, however, although quark constituents provide an economical explanation of strong interaction phenomena, no experiment has ever revealed evidence for an isolated quark, for instance via the observation of a fractionally-charged object on a Millikan oil-drop.

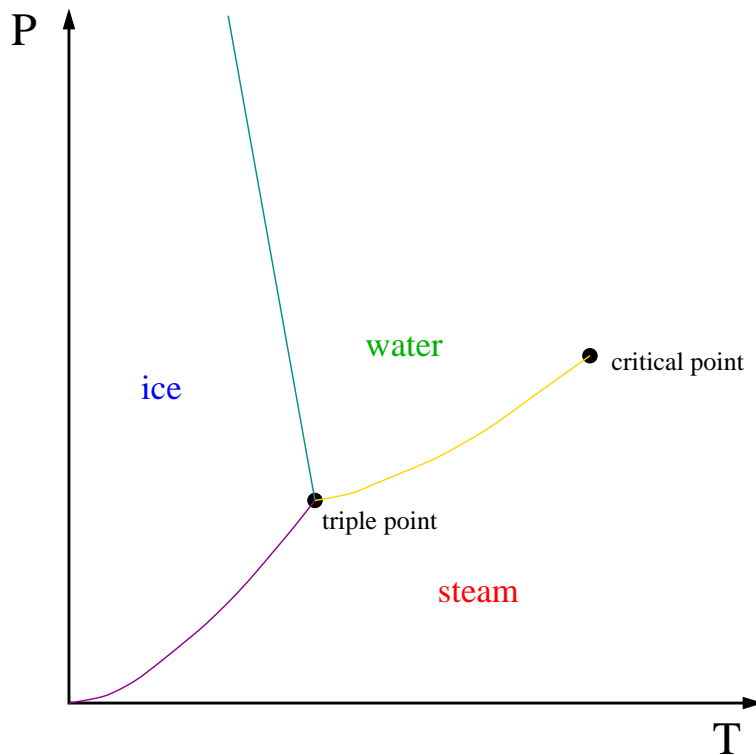


Figure 2: Phase diagram for H₂O (not to scale)

In this article I wish to explore the consequences of the quark picture for the thermodynamics of strongly-interacting matter, in other words, its behaviour as con-

ditions such as temperature and density are varied. Thermodynamical information is often presented in the form of a *phase diagram*, in which the different manifestations or phases of a substance occupy different regions of a plot whose axes are calibrated in terms of the external conditions or *control parameters*. The most familiar example, of course, is that of H₂O shown in Fig. 2; the control parameters are temperature T and pressure P , and the three regions correspond to the three phases of ice, water and steam. The lines mark the various coexistence curves $P(T)$ where two phases are in equilibrium; a phase transition such as melting or boiling is observed when moving along a path in the (T, P) plane which intersects such curves. Two special points in the diagram are the *triple point* ($T_{tr} = 273.16\text{K}$, $P_{tr} = 600\text{Nm}^{-2}$) where all three phases coexist, and the *critical point* ($T_c = 647\text{K}$, $P_c = 2.21 \times 10^7\text{Nm}^{-2}$), where the meniscus separating liquid from vapour disappears, and the two fluid phases become indistinguishable. For $T < T_c$ the transition between liquid and vapour is *first-order*, implying discontinuities ΔS and ΔV in entropy and volume respectively, and a non-vanishing latent heat and interface tension. This classification follows because entropy and volume are both first derivatives of the Gibbs free energy $G(T, P)$:

$$S = -\left.\frac{\partial G}{\partial T}\right|_P ; \quad V = \left.\frac{\partial G}{\partial P}\right|_T. \quad (1.1)$$

At the critical point the transition becomes *second order*, which means that singularities instead occur in specific heat C_P and isothermal compressibility κ_T of the fluid, which are related to second derivatives of the free energy:

$$C_P = -T \left.\frac{\partial^2 G}{\partial T^2}\right|_P ; \quad \kappa_T = -\frac{1}{V} \left.\frac{\partial^2 G}{\partial P^2}\right|_T. \quad (1.2)$$

In fact, each of the quantities in eqn.(1.2) diverges at the critical point. Another interesting phenomenon is *critical opalescence*: the size of droplets of the liquid phase within the vapour (or *vice versa*) becomes comparable with the wavelength of visible light, implying large optical path differences between adjacent parallel rays of light and hence strong scattering – the system thus becomes opaque near the critical point. Just beyond the critical point, thermodynamic observables still vary very rapidly as one moves about the (T, P) plane due to the large values of C_P and κ_T ; this is known as a *crossover region*.

Fig. 3 shows a proposed phase diagram for QCD. The names of the various phases are shown in green, and the environment in which they might be found in black. Phase coexistence lines are shown as solid lines, critical points as filled circles, and crossovers

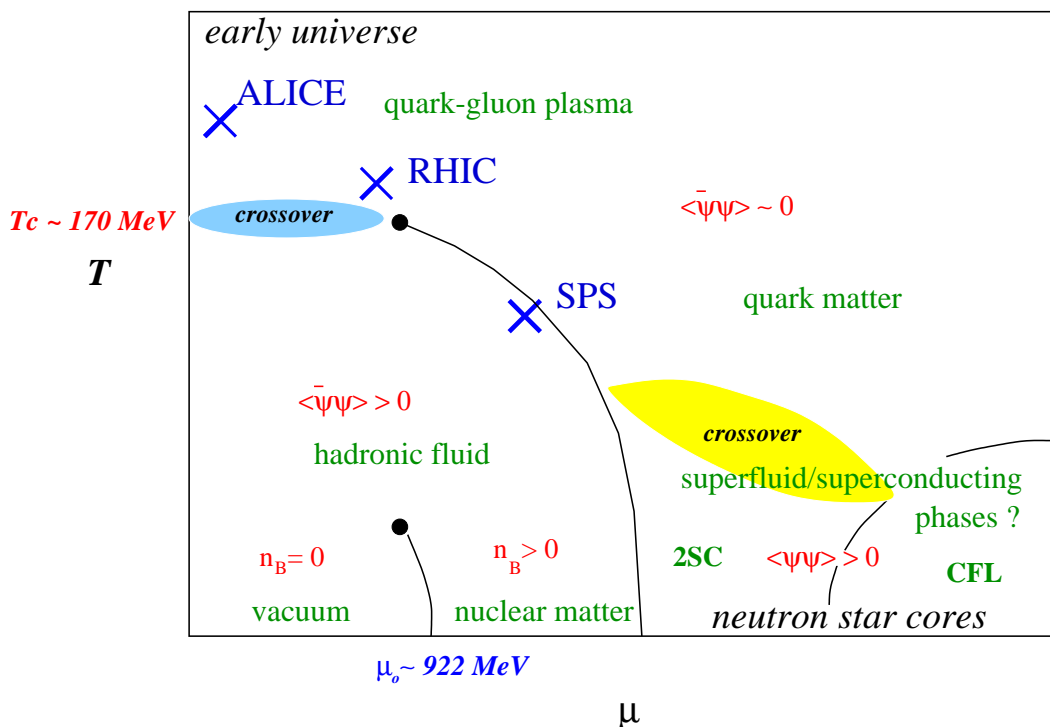


Figure 3: Proposed phase diagram for QCD. SPS, RHIC and ALICE are the names of relativistic heavy-ion collision experiments described in section 4. 2SC and CFL refer to the diquark condensates defined in eqns. (5.3,5.4).

by shaded regions. The control parameters are temperature T and *baryon chemical potential* μ , with which it is probably appropriate to (re-)familiarise ourselves. In particle physics reactions a qqq baryon is always created or destroyed pairwise with a $\bar{q}\bar{q}\bar{q}$ anti-baryon. There is no process within QCD which can change the number of baryons N_B minus the number of anti-baryons $N_{\bar{B}}$; in other words we can identify a conserved quantum number $B = N_B - N_{\bar{B}}$ called *baryon number*. Quarks and anti-quarks carry $B = \pm\frac{1}{3}$ respectively. Now, for systems in which baryon number is allowed to vary, the most convenient thermodynamic potential to consider is the *grand potential* $\Omega(T, V, \mu) = E - TS - \mu B$. Thermodynamic equilibrium is reached when Ω is minimised, and for a system in equilibrium we recognise μ as the increase in E whenever B increases by one. When systems are analysed using the *grand canonical ensemble* μ is kept as a control parameter, and the baryon density $n_B = B/V$ is a derived quantity whose value depends on the details of the equation of state $n_B = n_B(T, \mu)$.

It is worth making two further observations. Firstly, baryons are fermions and

are hence governed by the Pauli Exclusion Principle, implying that no two identical baryons can share the same quantum state. At $T = 0$ we thus expect baryonic matter to be *degenerate*, implying that energy states are fully populated up to some maximum energy called the Fermi energy E_F , in precise analogy with condensed matter systems such as electrons in a metal. For weakly interacting baryons μ coincides with E_F . Secondly, QCD is a relativistic quantum field theory, which means that in contrast with electronic systems the particles' rest-energy should be taken into account; we thus have $\mu = \mu_{NR} + m_0c^2$, where μ_{NR} is the non-relativistic chemical potential.

In the rest of this article I shall attempt to explain what is known about the phase diagram, giving quantitative details wherever possible. In the next section I will review QCD at zero temperature and chemical potential, paying particular attention to the question of why isolated quarks have not been observed, and why observed baryon masses are considerably greater than the u and d current quark masses shown in Table 1. In the bottom left-hand corner of the phase diagram where T and μ are both small the thermodynamic behaviour of QCD can be described in terms of a vapour of hadrons, which as we have seen are composite states of quarks and/or anti-quarks. The principal task for QCD theorists in this region is therefore to classify and quantify the bound states; there is a sense in which this can be caricatured as “relativistic atomic physics”. In section 3 I will use simple thermodynamic reasoning to argue that this state of affairs cannot persist as T is raised – eventually there comes a point where either a transition or a crossover occurs to a phase where the dominant degrees of freedom are no longer hadrons but the quarks themselves, together with other partons called *gluons*. Since quarks and gluons play similar roles in QCD to the electrons and photons of QED, this phase is often called the *quark-gluon plasma* (QGP), and QCD in the upper-left region of the diagram shares much terminology with relativistic plasma physics. In section 4 I discuss where the QGP might be observed; since the required temperatures turn out to be extraordinarily large, the only two candidates are the early universe, in the first instants following the Big Bang, and in high energy collisions between not elementary particles, but entire atomic nuclei which are first stripped of their attendant electrons and then accelerated to relativistic speeds. Such experiments are currently being performed at the Relativistic Heavy Ion Collider (RHIC) in Brookhaven National Laboratory, New York, and still more energetic ones are planned at the ALICE² detector at CERN in Geneva. Finally, I switch attention along the μ -axis, where very little is known beyond the onset of

²A Large Ion Collider Experiment

nuclear matter at $\mu_o \simeq 922\text{MeV}$, given by the nucleon rest mass minus the binding energy per nucleon, which is estimated from empirical models of nuclei such as the liquid drop model. Once again, there is believed to be a phase transition at a larger value of μ to a phase in which quarks rather than nucleons are the dominant degrees of freedom. Such *quark matter* may conceivably be found at the cores of compact astrophysical objects such as neutron stars. The nature of quark matter has recently been the focus of intense theoretical interest; it has been speculated that Fermi surface phenomena analogous to the Bardeen-Cooper-Schrieffer (BCS) instability, responsible for superconductivity in metals and superfluidity in liquid ${}^3\text{He}$ at low temperatures, may play an important role. In the lower-right region of the phase diagram, therefore, QCD becomes a branch of condensed matter physics.

2 Vacuum QCD

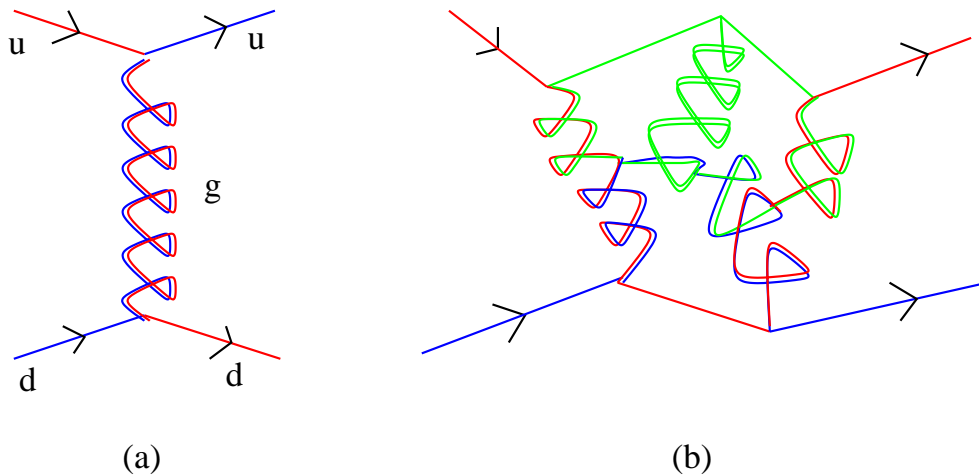


Figure 4: Gluon exchange between quarks. For small inter-quark separation, single gluon exchange (a) dominates. For larger separations gluon self-interactions (b) are also important.

The fundamental interaction between quarks in QCD arises from the exchange of spin-1 particles called *gluons* g , shown schematically in Fig. 4. Gluons are present inside hadrons and are thus also partons, but carry zero baryon number. Their existence is indirectly confirmed by the observation of particle collisions from which 3 jets emerge, one of which must result from a high-energy gluon formed in the initial collision, subsequently decaying into a group of hadrons with net $B = 0$.

The prototype for the quark-gluon interaction is provided by a theory called Quantum Electrodynamics (QED), which describes the force between electrically-charged particles such as electrons in terms of exchange of massless neutral quanta of the electromagnetic field, namely photons. It can be shown that the force between two charges due to the single photon exchange process analogous to that shown in Fig. 4a is described by a potential

$$V(r) = \frac{A}{r}, \quad (2.1)$$

where A is proportional to the product of the charges; in other words, single photon exchange reproduces the Coulomb potential, and the resulting lines of electric flux between equal and opposite charges trace out the familiar dipole field pattern, shown in Fig. 5. In QCD the corresponding quantity is called *chromoelectric flux*, and the

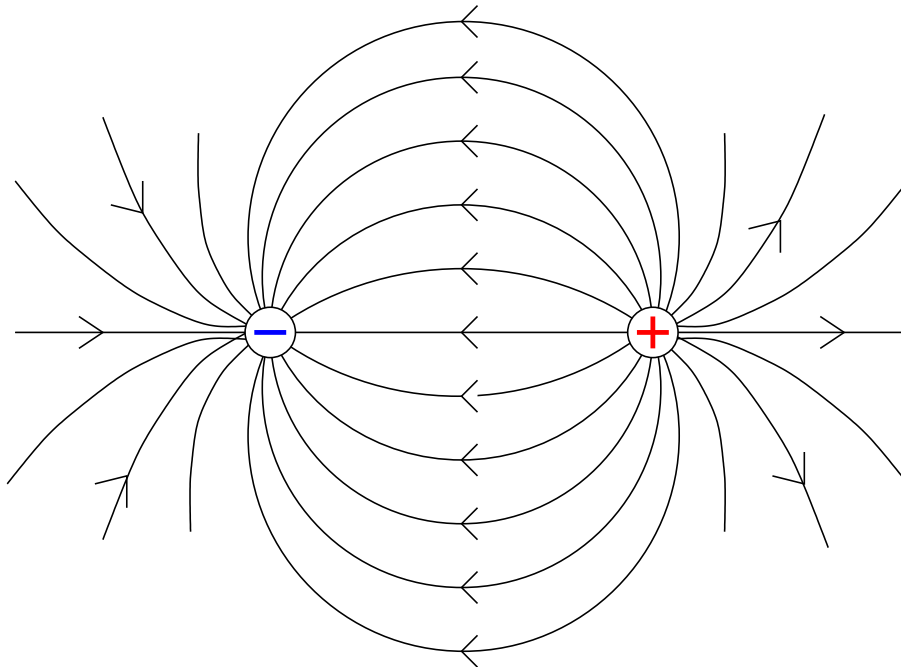


Figure 5: Lines of electric flux between a pair of equal and opposite electric charges.

gluon is the quantum of the chromoelectric and chromomagnetic fields. By contrast with QED, however, single gluon exchange in QCD only gives an accurate description of the force between quarks at very small distances. At larger separation, things become much more complicated because as well as interacting with q and \bar{q} , gluons can interact with themselves (as explained below; see also Fig. 4b), in contrast to photons which are electrically neutral and hence do not self-interact. The gluons'

additional “stickiness” presents a theoretical challenge which to date has had no completely satisfactory solution; indeed, most of our quantitative knowledge about the quark-gluon interaction at distance scales $\gtrsim O(0.5\text{fm})$ comes from formulating the equations of QCD on a discrete mesh of spacetime points and modelling quantum fluctuations of the q , \bar{q} and g fields by numerical simulation. A measure of the difficulty of this problem is that such *lattice gauge theory* simulations require dedicated use of the world’s most powerful computers [3]. Here we content ourselves with summarising the result: it turns out that the potential between a $q\bar{q}$ pair at separation r is

$$V(r) = -\frac{A(r)}{r} + Kr. \quad (2.2)$$

For small r the first term in (2.2) dominates, and describes an attractive Coulomb-like interaction. It is important to note, however, that the coefficient A itself has a mild scale-dependence due to quantum effects. Detailed analysis reveals that $A(r) \propto 1/\ln(r^{-1})$, implying that the interaction between quarks gets weaker as their separation decreases. In the limit $r \rightarrow 0$ the quarks can be considered non-interacting, a property known as *asymptotic freedom* [4]. Asymptotic freedom enables inelastic electron-proton collisions to be interpreted in terms of scattering of high-momentum virtual photons off almost-free partons; its theoretical discovery thus played a pivotal role in establishing QCD as the theory of the strong interaction.

As r increases the second term in (2.2) takes over, implying that the $q\bar{q}$ potential rises linearly with separation. This can be understood by considering Fig 6, which

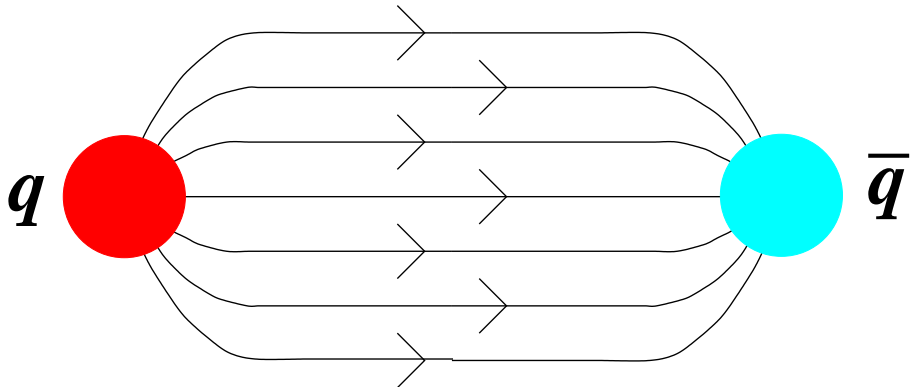


Figure 6: Chromoelectric flux between a $q\bar{q}$ pair.

shows lines of chromoelectric flux between a quark and anti-quark. By contrast with QED, the field lines do not spread out in space to form a dipole pattern, but remain

localised within a narrow region of diameter $\sim 0.7\text{fm}$ between the sources known as a *fluxtube* [5]. Within the tube the chromoelectric field strength is roughly uniform; therefore the energy of the system is proportional to the length of the fluxtube, in agreement with eqn.(2.2). In other words, the $q - \bar{q}$ force in this regime does not diminish with distance. In this picture it is appropriate to consider hadrons as little pieces of spinning chromoelectric “string”, whose ends are defined by the q, \bar{q} moving at relativistic speeds. By matching the masses of the various observed hadrons against their angular momentum (which of course is quantised in units of \hbar), it is possible to estimate the coefficient K in (2.2). Since it has units of energy per unit length, it is known as the *string tension*, with value $\simeq 880\text{MeV}/\text{fm} \simeq (420\text{MeV})^2$,³ ie. a force sufficient to lift three elephants!

At first sight eqn.(2.2) suggests that the energy required to effect complete separation of the quarks, that is, to “ionise” a hadron, is infinite. This is not strictly true, because at some point the application of a non-relativistic concept such as $V(r)$ to relativistic quarks must break down. Once the energy stored in the flux tube becomes comparable to twice the rest-energy of a quark, it becomes possible to break the string by $q\bar{q}$ pair-production, the new particles acting as a fresh sink or source for the broken flux lines. The result is two $q\bar{q}$ mesons, each with a smaller interquark separation than the original energetic meson. This process of particle production via string-breaking helps to explain the profusion of hadrons formed in high-energy collisions.

Let us develop the analogy with QED a little further. The QCD quantity corresponding to electric charge is called *color*, and comes in three forms: “red”, “blue” and “green”. Both quarks and gluons have color quantum numbers. Anti-quarks have complementary colors “anti-red” (shown as cyan in Fig. 6), “anti-blue” and “anti-green”. The gluon exchange responsible for QCD forces carries color between different particles; hence the colored nature of the gluons can be regarded as the origin of their self-interaction. As well as providing the theory with its name, the slightly frivolous terminology conveys in a heuristic way a deep dynamical principle of QCD. Suppose we denote a green quark, for instance, by q_g ; the only stable finite-energy systems are those formed from complementary combinations of color, such as $q_g\bar{q}_g$ mesons or $q_r q_b q_g$ baryons. The $q\bar{q}$ pair formed in string-breaking is produced with

³In particle physics it is conventional to use units in which $\hbar = c = 1$, in which case energy, momentum and mass are all measured in the common unit MeV, and distance and time, via the expression for the Compton wavelength $r = ct = \hbar/mc$, in units of $(\text{MeV})^{-1}$. A useful conversion factor is $1\text{fm} \simeq (200\text{MeV})^{-1}$.

exactly the right color combination to maintain this overall color-neutrality. Forces between color-neutral objects such as nucleons within the nucleus can be viewed as a second-order effect akin to Van der Waals forces between neutral atoms.⁴ From our viewpoint the most important aspect is that colored objects such as isolated quarks or gluons are never observed. This property of QCD, supported by all the theoretical considerations of the previous paragraphs, and to date not contradicted by experiment, is called *color confinement*.

While a complete quantitative description of hadrons in QCD remains elusive, for many practical purposes including the thermodynamic arguments to be developed in the next section, a simplified treatment is both possible and desirable. The two crucial ingredients we have identified, asymptotic freedom and color confinement, are built into a much simpler description of the strong interaction known as the *Bag model*, in which massless quarks move freely within a spherical hadron of radius R , but are prevented from travelling further by an inwards-acting pressure due to the confining nature of the bulk vacuum [6]. This can be modelled by assigning a constant energy density Λ_B^4 to the non-confining region within the hadron. The energy of a hadron of radius R is then given by

$$E \sim R^3 \Lambda_B^4 + \frac{C}{R}, \quad (2.3)$$

the second term arising from the kinetic energy of the confined quarks due to the Uncertainty Principle. The hadron mass can be found by minimising E with respect to R ; eliminating the constant C one finds

$$M \sim 4R^3 \Lambda_B^4. \quad (2.4)$$

Using typical values $M \sim 1000\text{MeV}$, $R \sim 1\text{fm}$, we derive a value for the bag constant $\Lambda_B \sim 200\text{MeV}$.

We now come to another important aspect of QCD dynamics. When a particle with spin \vec{s} propagates, it is possible to define a quantity called *helicity* $h = \vec{s} \cdot \vec{k} / |k|$, which is the projection of the spin axis along the direction of the particle's motion, defined by the momentum \vec{k} . For a spin- $\frac{1}{2}$ particle like the quark, there are two possible helicity eigenstates $h = \pm\frac{1}{2}$, usually referred to as left- and right-handed states since they are related by a mirror reflection. A quark's helicity is not altered by either emission or absorption of a gluon; hence in the absence of any other effect one might deduce that the numbers of left- and right-handed quarks are separately

⁴In fact inter-nucleon forces can be modelled by the exchange of color-neutral mesons such as pions. The dimension of a nucleus is comparable with the Compton wavelength of a pion.

conserved in QCD, leading to two good quantum numbers B_L and B_R . A moment's thought, however, shows that this can only be the case if quarks have zero mass and hence travel at the speed of light. Otherwise, it is possible to Lorentz boost to a frame in which the quark's momentum has the opposite sign; since angular momentum along the boost axis is not changed, helicity in the new frame must also have the opposite sign. We conclude that in a relativistically covariant treatment massive quarks must be described as a superposition of helicity eigenstates, the mass m parametrising the overlap between them and hence effectively the rate of $L \leftrightarrow R$ transitions. Since in this case only $B = B_L + B_R$ remains as a good quantum number, we say that the *chiral symmetry* relating left and right-handed quarks and enabling them to be thought of as independent particles is broken by the quark mass.

Chiral symmetry breaking (χ SB), like that of other symmetries in many-body or quantum field theory, can occur via the theory's own dynamics. We have seen that QCD is responsible for a strong attractive interaction between q and \bar{q} . The force is so strong, in fact, that the state usually considered as the ground state or *vacuum*, namely that of no particle present, is actually unstable with respect to formation of a *condensate* of tightly bound $q\bar{q}$ pairs, much as the ground state of superfluid helium is a Bose condensate of He atoms in the lowest quantum state. Let us denote the vacuum by the ket $|0\rangle$, and the field operators which create or destroy a quark when acting on a ket as $\bar{\psi}, \psi$ respectively. A χ SB vacuum is then given by

$$\langle \bar{\psi}\psi \rangle \equiv \langle 0 | \bar{\psi}_L \psi_R + \bar{\psi}_R \psi_L | 0 \rangle \neq 0. \quad (2.5)$$

Since neither $|0\rangle$ is annihilated by ψ , nor $\langle 0|$ by $\bar{\psi}$, the vacuum must contain $q\bar{q}$ pairs. In QCD it is believed that the value of $\langle \bar{\psi}\psi \rangle \simeq (250\text{MeV})^3$, which can be interpreted as the number of such pairs per unit volume.

As eqn.(2.5) implies, the condensate pairs ψ_L with $\bar{\psi}_R$, and *vice versa*. Since $\bar{\psi}\psi$ leaves $B_L + B_R$ invariant but changes $B_L - B_R$ by two units, a non-vanishing condensate implies that the latter quantity has no definite value in the vacuum and only B remains as a good quantum number. A left-handed quark propagating through such a vacuum can be annihilated by ψ_L , leaving $\bar{\psi}_R$ to create a right-handed quark with the same momentum. The quark will thus flip its helicity at a rate proportional to $\langle \bar{\psi}\psi \rangle$ – in other words, it will propagate just as if it had a mass. We refer to this dynamically-generated mass as the quark's *constituent mass* Σ , as opposed to the quark's intrinsic or *current mass* m . If χ SB occurs spontaneously by the formation of a large $\langle \bar{\psi}\psi \rangle$, then Σ may be very much greater than m due to this dynamical mass

generation. We have listed estimates of both values for the known quarks in Table 1, although since isolated quarks are not observed, neither quantity is unambiguously defined. If we look at the values for the u and d quarks, however, we see that $m_{u,d}$ is not very much larger than the electron mass 0.511MeV , whereas $\Sigma_{u,d}$ is comparable to one-third the nucleon mass 940MeV .

Spontaneous χSB in QCD is thus the agency by which the nucleon (and by extension the universe as a whole) acquires most of its mass. It is also a natural consequence of quark confinement [7]. Consider the bag model description of massless quarks moving back and forth within a small volume. At the surface of the bag the quarks must reverse their direction of travel, but not their angular momentum, which is always conserved. Therefore the interaction with the bag wall changes their helicity. Since this cannot be achieved through any process involving gluon exchange between the quarks in the bag, it must arise because the QCD vacuum in the volume outside the bag contains a non-vanishing density of $q\bar{q}$ pairs with which the bag quarks can exchange helicity. Confinement implies χSB .

A useful analogy for χSB is supplied by the phenomenon of ferromagnetism in metals. On each atom of the metal, occupying a site of a regular crystal lattice, there is an unpaired electron carrying a magnetic moment or “spin” conveniently denoted by \uparrow . Quantum mechanical exchange forces dictate that there is a tendency for spins on adjacent sites to align, although the preferred direction of alignment (ie. $\uparrow\uparrow$ vs. $\downarrow\downarrow$) is not determined by the microscopic Hamiltonian. However, if the temperature is low enough (ie. $T < T_c$, the Curie temperature), then cooperative interactions amongst spins at arbitrary separation result in a ground state in which a macroscopic fraction of the spins is aligned, resulting in the spontaneous magnetisation of the sample $M = \langle \uparrow \rangle \neq 0$ (angled brackets here denote a thermodynamic average rather than a quantum expectation value). Since the magnetisation axis defines a particular direction in space, the original symmetry of the Hamiltonian under rotations of the spin axis is spontaneously broken by $M \neq 0$. The same effect can be promoted by an external magnetic field $h \neq 0$, which in this case explicitly breaks the symmetry. The relation between M and h exactly mirrors that between $\langle \bar{\psi}\psi \rangle$ and m in QCD.

It is interesting to examine the spectrum of excitations above the ferromagnetic ground state $M \neq 0$; it turns out that coherent oscillations of the spins in directions orthogonal to the magnetisation axis, known as *spin-waves*, cost arbitrarily small amounts of energy to excite in the limit of wavenumber $k \rightarrow 0$. Spin-waves due to χSB in QCD correspond to massless bosonic particle excitations, which are identified

with the pion triplet π^\pm, π^0 . With masses 135 - 140MeV, these are by far the lightest hadrons, the next lightest meson made from u, d quarks being the ρ at 770MeV, and lightest baryon being the proton at 938MeV. The π is not exactly massless due to the explicit χ SB introduced by $m_{u,d} \neq 0$.⁵ The π plays a special role in QCD – its lightness provides the most direct evidence for a vacuum with χ SB, and many of its interactions were predicted purely on symmetry grounds alone, long before the dynamics of QCD were worked out in any detail, or the theory even formulated.

3 The Quark-Gluon Plasma

A natural consequence of the composite nature of hadrons in QCD is that there should be a phase transition as temperature T is raised. Let us start by considering QCD with just u and d quarks, and ignoring the heavier flavors. If there is no net concentration of baryons (ie. $B = \mu = 0$), then the dominant hadronic degrees of freedom in a hot medium are initially pions π^\pm, π^0 , which carry zero B and can be relatively easily pair-produced. If we neglect their rest mass, which is accurate for $T \gtrsim 100\text{MeV}$,⁶ then the pressure due to a pion gas is given by adapting the formula for blackbody radiation pressure:

$$P_\pi = -\left.\frac{\partial\Omega_\pi}{\partial V}\right|_{T,\mu} = 3 \times \left(\frac{\pi^2}{90}\right) T^4, \quad (3.1)$$

the factor three counting the number of pion charge states. Now, the equivalent expression for a plasma of free light quarks and massless gluons which are no longer confined within hadrons is much larger, because there are so many more degrees of freedom (ie. the plasma is a state of higher entropy):

$$P_{q\bar{q}} = 2 \times 2 \times 3 \times \frac{7}{4} \times \left(\frac{\pi^2}{90}\right) T^4 \quad ; \quad P_g = 2 \times 8 \times \left(\frac{\pi^2}{90}\right) T^4. \quad (3.2)$$

The numerical factors require explanation: for $q - \bar{q}$ pairs there are 2 helicity states each, 2 flavor states (u and d), and 3 color states. The factor $\frac{7}{4}$ arises due to the difference between Fermi-Dirac and Bose-Einstein statistics. For g , there are 2 helicity states and 8 color states (this is because gluons carry a combination of color and anti-color). Now, naively we expect the hadron gas and quark-gluon plasma to be in

⁵Arguments based on general features of chiral symmetry breaking relate the pion mass to its size via $M_\pi \sim R_\pi \sqrt{m_{u,d} \langle \bar{\psi}\psi \rangle}$.

⁶We also use units in which Boltzmann's constant $k_B = 1$. A useful conversion is $1\text{MeV} \simeq 10^{10}\text{K}$.

equilibrium when the pressures coincide; however we must also take confinement into account, most easily by considering the bag constant of the previous section to act as a *negative pressure* for the QGP [8]. We arrive at

$$\frac{1}{30}\pi^2 T_c^4 = \frac{37}{90}\pi^2 T_c^4 - \Lambda_B^4, \quad (3.3)$$

whence the critical temperature for plasma formation, when the quarks are released from their confinement, is $T_c \simeq 144\text{MeV}$, somewhat over a trillion kelvin! The energy density of the plasma phase is predicted to be $\varepsilon_{QGP} \simeq 850\text{MeV}/\text{fm}^3$, and the latent heat at the transition $\Delta\varepsilon \simeq 800\text{MeV}/\text{fm}^3$.

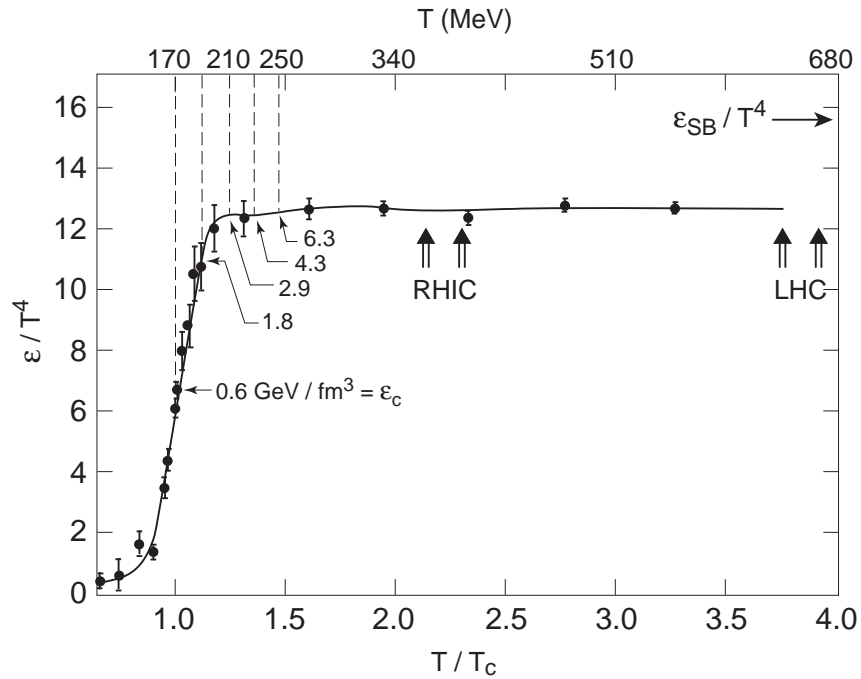


Figure 7: Energy density ε/T^4 vs. temperature T/T_c for QCD with 3 light quark flavors. Heavy ion collisions at CERN’s Super Proton Synchrotron probe energy densities in the neighbourhood of the “knee” of the curve, as described in Section 4. RHIC and LHC refer to the regimes attainable at the Relativistic Heavy Ion and Large Hadron Colliders. (courtesy F. Karsch)

The model we have used is crude, in effect treating the inside and outside of the bag as different phases. More refined calculations of the transition to the QGP are

made using the lattice gauge theory techniques mentioned in the previous section. In Figs. 7, 8 and 9 we show the results of recent calculations performed on QCD with varying numbers of light quark flavors [9]. Fig. 7 shows the energy density ε , and Fig. 8 the pressure P as functions of T . Each is expressed as a fraction of T^4 , enabling comparison with the Stefan-Boltzmann predictions (3.2) together with $\varepsilon_{SB} = 3P_{SB}$, valid for a non-interacting relativistic plasma. Fig. 7 shows the energy

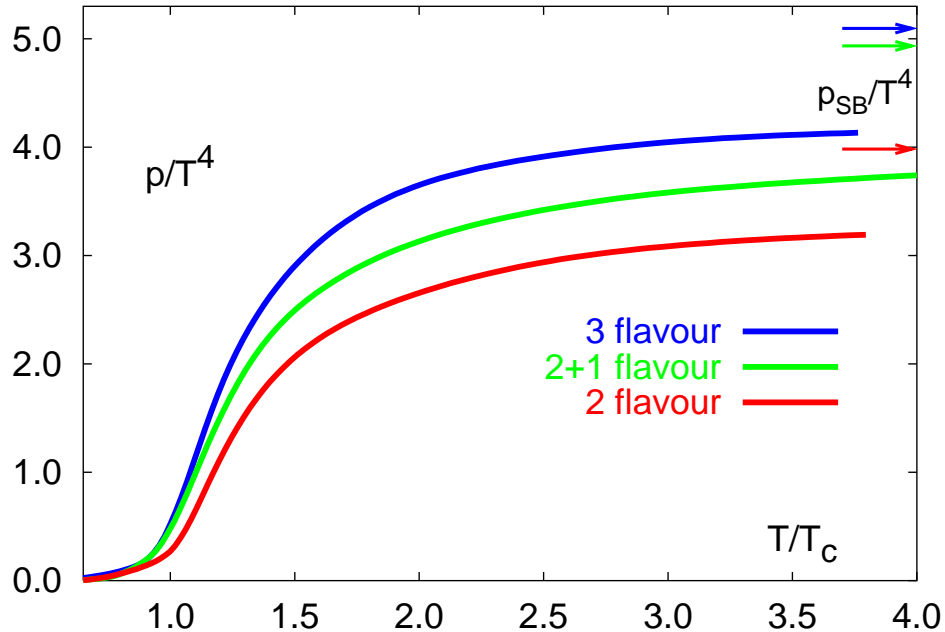


Figure 8: Pressure P/T^4 vs. temperature T/T_c for 2, 2+1 and 3 flavor QCD. (courtesy F. Karsch)

density rising very steeply at $T \simeq 170\text{MeV}$, and rapidly reaching a plateau at roughly 80% of the SB value. This is strong evidence for QGP formation at $T_c \simeq 170\text{MeV}$, $\varepsilon_c \simeq 600\text{MeV}/\text{fm}^3$, in rough agreement with the bag model estimates. The disparity between the high- T phase and a non-interacting plasma, however, is reinforced by Fig. 8, which shows that for $T \lesssim 3T_c$ the pressure falls appreciably below the SB value. Strong interactions between q , \bar{q} and g persist in the QGP. Only at very high temperatures when large energies are exchanged in inter-particle collisions will the interaction strength weaken due to asymptotic freedom, making calculations using the single gluon exchange approximation feasible.

How else can the QGP be characterised? Fig. 9 shows the chiral condensate $\langle \bar{\psi}\psi \rangle$

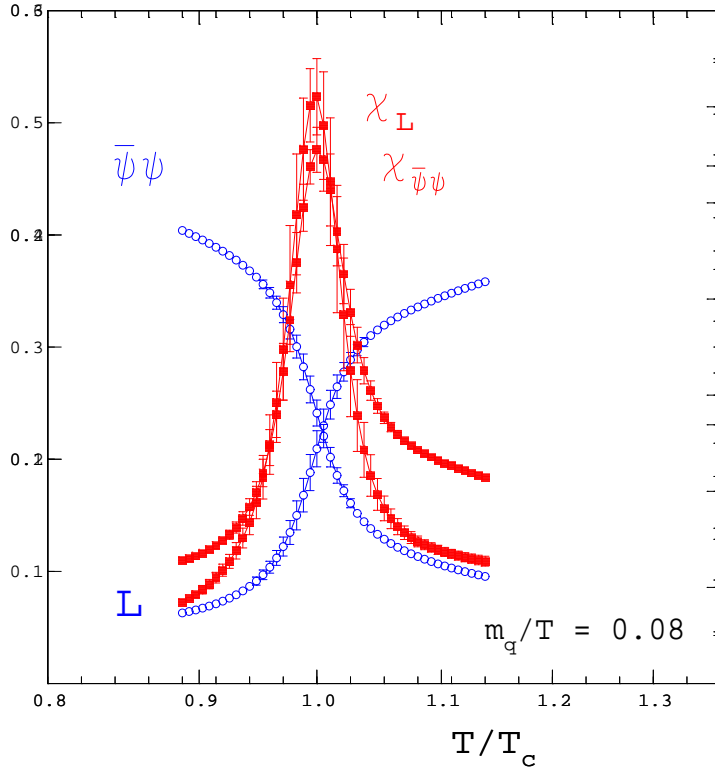


Figure 9: Chiral condensate $\langle \bar{\psi}\psi \rangle$ and quark free energy function $L(f_q)$ as functions of T in the neighbourhood of the transition (blue), together with their associated susceptibilities (red). (courtesy F. Karsch)

as a function of T , together with a quantity L related to the free energy $f_q(T)$ of an isolated quark via $L \propto \exp(-f_q/T)$. For $T < T_c$ $\langle \bar{\psi}\psi \rangle$ is large signalling χ_{SB} , and L is small, signalling that the energy of an isolated color source diverges, ie. confinement. Across the transition this behaviour reverses itself indicating both that *chiral symmetry is restored* and that *color is no longer confined* in the QGP. Also shown are the associated *susceptibilities* defined by $\chi_L = \langle L^2 \rangle - \langle L \rangle^2$, and analogously for $\chi_{\bar{\psi}\psi}$. These quantities indicate how strongly thermodynamic observables fluctuate, and, as second derivatives of the free energy, peak or even diverge at a phase transition. It is a remarkable fact that these two *a priori* distinct transitions appear to coincide, as revealed by the merging of the peaks in Fig. 9.

The dominant degrees of freedom in the QGP are thus light q , \bar{q} and g , which justifies in retrospect the bag model treatment used previously. In terms of the $q\bar{q}$ potential (2.2), the QGP is characterised by the vanishing of the string tension K ;

indeed, V now takes a different form:

$$V_{QGP}(r) = -\frac{C}{r} \exp(-r/\lambda_D), \quad (3.4)$$

where $\lambda_D(T) \propto 1/T$ is the *Debye screening length* due to the non-zero density of naked color sources in the QGP. For $T \gtrsim T_c$ $\lambda_D \sim O(0.1\text{fm})$ [10].

The value found for T_c justifies the neglect of the heavy quarks c , b and t in QCD thermodynamics, since their equilibrium concentration remains heavily suppressed by the Boltzmann factor $\exp(-m_{c,b,t}/T)$ in the critical region. We can thus restrict our attention to u , d and s . In the limit $m_{u,d} \rightarrow 0$ $\langle \bar{\psi}\psi \rangle$ can be regarded as an *order parameter* which vanishes in the QGP, just like the magnetisation M of a ferromagnet which vanishes at the Curie point. We have thus labelled “hadronic” and QGP phases in Fig. 3 by the value of $\langle \bar{\psi}\psi \rangle$ (shown in red). Another legitimate question is the order of the phase transition; the large latent heat predicted by the bag model indicates a strong first order transition. However, our simple treatment has ignored any possible variation with temperature of the bag constant Λ_B itself. In fact, lattice calculations with 3 light quark flavors reveal $\Delta\varepsilon$ to be much smaller than the bag prediction and hence the first-order transition much weaker; $\Delta\varepsilon$ may even vanish altogether if m_s is sufficiently large, ie. the transition is actually second order for just two light flavors [11]. Now, since $m_{u,d} \neq 0$ the order parameter $\langle \bar{\psi}\psi \rangle$ strictly never vanishes, but rather drops steeply in the transition region. For this reason we have indicated QGP formation along the $\mu = 0$ axis in Fig. 3 as a crossover rather than a true phase transition, with a possible critical point ending a line of first-order transitions somewhere within the (T, μ) plane. It should be stressed, however, that further numerical work is needed before this picture can become conclusive.

4 Relativistic Heavy-Ion Collisions

Having discussed the reasons for supposing that a new state of strongly-interacting matter exists, we should now consider how it might be observed, which translates into the question of where to find or how to produce temperatures of $O(10^{12}\text{K})$. A natural place to look is immediately after the Big Bang, when the energy density in the early universe considerably exceeded any found naturally today. In the first moments, energies were so high that all matter was highly relativistic; under these circumstances integration of the Friedmann equations governing the universe’s expansion predicts that the radius R of the observable universe is related to the time after the Big Bang t

and temperature T via $R \propto T^{-1} \propto t^{\frac{1}{2}}$; at later times when matter cooled and became non-relativistic the behaviour changed over to $R \propto t^{\frac{2}{3}}$. We can use this information to extrapolate back from present conditions to predict that the QGP last existed between 10^{-5} and 10^{-4} s after the Big Bang. This is beyond the range of direct observation, which cannot penetrate beyond the epoch when the cosmic microwave background radiation was formed at roughly $t \sim 10^5$ years. The transition from quarks to hadrons may have left a footprint, however, if it were first order. In this case, because of the non-zero interface tension between the phases, the transition would have proceeded inhomogeneously, eg. via the growth of bubbles of the hadronic phase at isolated points within the QGP. This would have resulted in local fluctuations in baryon concentration, which possibly had a significant impact on the relative abundances of light elements formed at the nucleosynthesis epoch at $t \sim 10$ minutes [12].

In recent years, however, most attention has focussed on the possibility of recreating the QGP in terrestrial laboratories in *relativistic heavy-ion collisions*, ie. high energy collisions between nuclei such as sulphur (S), lead (Pb) and gold (Au) [13]. The first experiments have been performed with fixed target nuclei at the Alternating Gradient Synchrotron (AGS) in Brookhaven and the Super Proton Synchrotron (SPS) at CERN, with centre of mass (CM) energies of $2A$ and $18A$ GeV respectively (A is the number of nucleons in the nucleus). Last year experiments with colliding nuclear beams commenced at RHIC in Brookhaven, taking advantage of the higher energy of $200A$ GeV available in the CM frame; experiments are due to start at the ALICE detector at the Large Hadron Collider (LHC) at CERN in 2006, this time with a CM energy of $5500A$ GeV. The regions of the phase diagram probed by these experiments are indicated schematically by blue crosses in Fig. 3. The collisions are incredibly complex events, producing $O(10^3)$ charged particle tracks at SPS and RHIC energies and forecast to produce $O(10^4)$ at ALICE, and their study presents a stringent challenge to data acquisition and storage techniques. An end-on view of the charged tracks, ie. viewed along the beam, from a recent event observed at the STAR detector at RHIC is shown in Fig. 1.

The various stages of a heavy-ion collision are portrayed in Fig. 10. The colliding nuclei are envisaged as spherical in their rest frame, but in the CM frame are Lorentz-contracted along their direction of motion due to their relativistic velocity $\beta = v/c$: even at SPS energies the length contraction factor $\gamma(\beta) \simeq 10$, so the nuclei are best pictured as “pancakes” (see Fig. 10a). When the nuclei meet, the initial events are high-energy inelastic collisions between individual nucleons, in which many partons

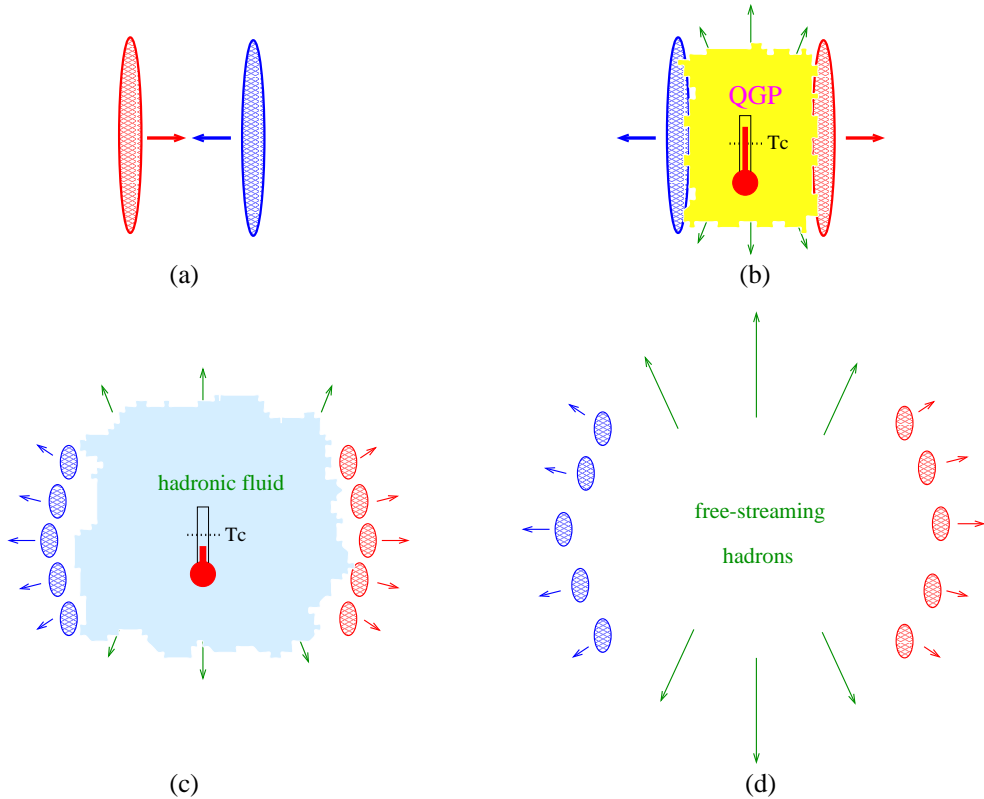


Figure 10: Schematic view of the various stages of a heavy-ion collision. The thermometers indicate when thermal equilibrium might be attained.

are liberated. Because the density of nuclear material is high, the released partons have the opportunity to rescatter several times with the result that their momenta, initially highly correlated along the beam axis, are redistributed and a substantial fraction of the incident kinetic energy is deposited in the CM frame to produce a “fireball” in the *mid-rapidity* region $y \simeq 0$.⁷ This energy is then available for conversion to hadrons via $q\bar{q}$ pair production – for this reason as many anti-baryons as baryons will be produced in the mid-rapidity region, which thus has a net baryon density $n_B \simeq 0$, whereas the forward and backward regions $|y| \gtrsim 1$ (at SPS energies [14]), shown in red and blue in Fig. 10, are relatively rich in baryons corresponding to the initial concentrations in the nuclei which have in effect “passed through” each other.

⁷ For a particle with 4-momentum (E, \vec{k}) , the rapidity y of a collision product is defined by $y = \frac{1}{2} \ln \left(\frac{E+k_z}{E-k_z} \right)$, z being the direction along the beam axis. Rapidity is a convenient variable in the study of relativistic collisions since under Lorentz boosts it simply changes by an additive constant.

A question then presents itself: is the energy density ε produced in the mid-rapidity region sufficient, assuming thermalisation, to effect a phase transition to the QGP? An important result to help assess this possibility is due to Bjorken [15]: for a collision at the origin $(t, z) = (0, 0)$ the energy density in the central region at proper time $\tau = \sqrt{t^2 - z^2}$ is given by

$$\varepsilon(\tau) = \frac{1}{\tau \mathcal{A}} \left. \frac{dE_{\perp}}{dy} \right|_{y=0}, \quad (4.1)$$

where \mathcal{A} is the transverse area of the incident nuclei and dE_{\perp}/dy denotes the *transverse* energy of the collision products (ie. excluding kinetic energy due to motion parallel to z) per unit of rapidity.⁸ For Pb+Pb collisions at SPS with zero impact parameter, we observe $\mathcal{A} \simeq 60\text{fm}^2$ and $dE_{\perp}/dy \simeq 200\text{GeV}$ at mid-rapidity [13, 16]. Let us assume that if thermalisation occurs it does so over a typical QCD timescale of $\tau_0 \sim 1\text{fm}/c$ (the time taken for light to traverse a nucleon); eqn.(4.1) then yields $\varepsilon \simeq 3\text{GeV}/\text{fm}^3$. A comparison with Fig. 7 suggests that a temperature $T \simeq 200\text{MeV}$ is reached, ie. the fireball is hot enough to form QGP, as shown in Fig. 10*b*.

If QGP is formed, it must quickly expand and cool due to its excess pressure with respect to the vacuum. At some point, therefore, T falls below T_c , and hadrons reform (Fig. 10*c*). At around this point the composition of the hadrons formed, the majority of which are pions, is fixed – this is known as *chemical freezeout*. The resulting hadronic gas continues to cool until interaction rates become insufficient to maintain thermal equilibrium in the expanding medium; this is known as *thermal freezeout*, from which point the hadrons are free to stream away to be detected (Figs. 1,10*d*). Information about conditions inside the fireball must be inferred from hadrons emitted from the *surface of last scattering* at thermal freezeout, just as conditions in the early universe must be inferred from observations of the microwave background. Evidence for thermalisation comes from analysis of the distribution of transverse mass $m_{\perp} = \sqrt{m_0^2 + k_{\perp}^2}$, which is found to be approximately Boltzmann $\exp(-m_{\perp}/T)$ for a variety of different hadron species. Particularly useful information is carried by pairs of identical particles such as $\pi^-\pi^-$. The wavefunction of such identical bosons must be symmetric with respect to exchange of momenta; the resulting correlation enables the size of the collision region to be inferred from the momentum spectrum of the emitted particles [13]. The principle is identical to the two-photon *intensity interferometry* used to estimate stellar diameters in astronomy [17]. The combined results of these analyses suggest a freezeout temperature $T \lesssim 100\text{MeV}$, at which point the last

⁸Note that the volume element $Adz = \tau \mathcal{A} \cosh y dy$.

scattering surface has radius $\sim 7\text{fm}$ and expansion velocity $\sim 0.6c$ [18], all of which are consistent with the estimate of the initial energy density obtained using eqn.(4.1).

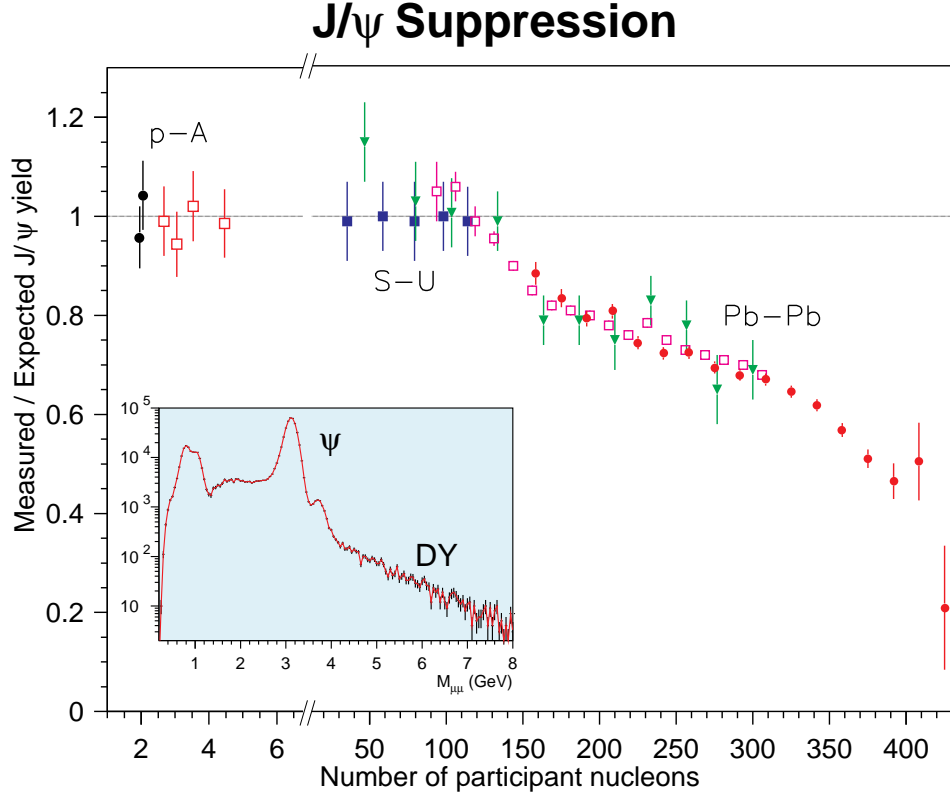


Figure 11: J/ψ suppression at the SPS. The data have been accumulated from proton-nucleus as well as sulphur-uranium and lead-lead collisions. The inset shows the number of muon pairs produced in an ion collision as a function of energy, clearly showing the peak due to J/ψ decay at $\sim 3\text{GeV}$, as well as a high energy tail due to the Drell-Yan (single photon exchange) mode of production. (courtesy C. Lourenço)

Since it is plausible that thermalisation occurs in heavy-ion collisions, and that the temperatures reached are of roughly the same order as T_c , it is legitimate to consider possible signals for QGP formation. The first is so-called J/ψ suppression [19]. Although charmed quarks are too heavy to be abundant in thermal equilibrium, they can be pair-produced in the initial high-energy collisions to form $c\bar{c}$ mesons, of which the J/ψ at 3097MeV is the lightest – in the vacuum it is relatively long-lived since it can only decay into lighter hadrons via an intermediate pure-gluon state which is hard to produce. Now, bound states of heavy quarks c, b, t are non-relativistic,

and the static potential $V(r)$ of eqn.(2.2) is much more appropriate for these systems than it is for mesons made from light quarks [20]. A consequence of QGP formation is that (2.2) is replaced by the screened potential (3.4): the $c\bar{c}$ pair will thus dissociate if the screening length λ_D falls below the analogue of the Bohr radius for the J/ψ . If this happens charmed quarks will be far more likely to form mesons with open charm such as the D ($c\bar{u}$, $c\bar{d}$), and hence fewer J/ψ mesons should be produced in heavy-ion collisions as compared to similar energy pp collisions. The number of J/ψ 's produced can be estimated via the fraction which decay not to hadrons but to pairs of muons $\mu^+\mu^-$. Muons are particles of mass 106MeV which do not feel the strong interaction; though unstable, they survive long enough to emerge from the fireball and be detected. A compendium of recent results is shown in Fig. 11 [21], where the suppression factor is plotted against the number of nucleons N_{part} participating in the ion collision, which is proportional to the energy density reached. Note that J/ψ suppression is expected even in the absence of QGP, due to dissociation on collision with other particles in a hadronic medium, and can be observed in pA collisions. This effect can be modelled by assuming a uniform decay rate integrated along the length of nuclear material traversed by the J/ψ before it emerges into the vacuum. The horizontal line in Fig. 11 is normalised to this model expectation; there is anomalous suppression for $N_{part} \geq 130$, which is strong evidence for quark-gluon plasma formation.

Another striking observation, *strangeness enhancement*, comes from analysing the relative abundances of hadron species in the collision products; it is found that many more hadrons containing s and \bar{s} quarks are produced in ion collisions than in similar energy pp or pA collisions. Data from the WA97 experiment at the SPS (Fig. 12) show enhancement factors for Λ (uds), Ξ (ssd) and Ω (sss) baryons and their corresponding anti-baryons, showing that eg. Ω production is enhanced by a factor of 17 for ion collisions with $N_{part} \geq 10^2$ [22]. What is the origin of this effect? It has been proposed that $s\bar{s}$ pairs will be much easier to produce in the QGP than in a hadronic medium [23], both because they are considerably lighter due to chiral symmetry restoration, and because of the much higher density of gluons, which opens up new formation processes such as gluon fusion $gg \rightarrow s\bar{s}$. Note that the current mass m_s is very similar in magnitude to T_c , which means that strangeness production should be a very sensitive function of T near the transition. Experiments currently under way at the NA57 detector at SPS will explore intermediate values of N_{part} , in the hope of finding a threshold for this effect.

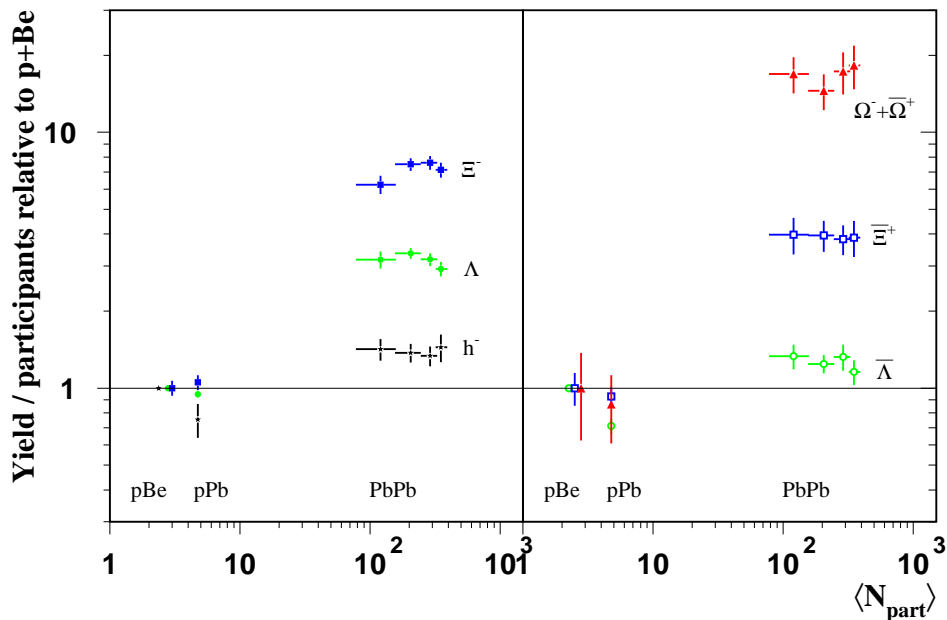


Figure 12: Evidence for strangeness enhancement from the WA97 experiment at CERN. (courtesy WA97 Collaboration)

Heavy-ion collisions at the SPS have yielded signals not easily explained in terms of purely hadronic physics. If the QGP has been seen, however, its lifetime is probably $O(1\text{fm}/c)$, comparable with the time taken for its formation following thermal equilibration. The current experiments at RHIC promise to produce QGP's at $T \simeq 400\text{MeV}$, with 4 times this lifetime, those at ALICE perhaps up to 10 times, making possible a detailed study of the QGP independent of artifacts induced by the proximity of the phase transition. Interpretation of J/ψ suppression (and the equivalent phenomenon in the Υ family of $b\bar{b}$ systems), and strangeness enhancement should become more clear-cut; additional observations such as thermal photon emission (ie. blackbody radiation) directly from the QGP will become feasible. Higher energies will also create jets, and their interaction with and penetration of the plasma will yield much important information. Finally, improved detector techniques will enable more detailed study of other thermal effects, such as the downward shift and broadening of the ρ meson resonance [24], due respectively to partial chiral symmetry restoration and collision-broadening⁹ in a hot hadronic medium. In more ways than one,

⁹This is analagous to the pressure broadening of spectral lines in atomic physics; the resonance width Γ is related to the ρ lifetime $\Delta\tau$ via the Uncertainty Principle $\Gamma \sim 1/\Delta\tau$, and hence increases

heavy-ion physics is entering a golden age.

5 Quark Matter and Color Superconductivity

I now consider the behaviour of QCD as a function of chemical potential μ . For T strictly zero as μ increases, the ground state is initially the state with no particle present, ie. the vacuum. This situation persists until μ reaches the value of the nucleon rest mass minus the binding energy per nucleon in nuclear matter, when it becomes energetically preferable to populate the ground state with a bound nucleon fluid. Ignoring Coulomb repulsive forces between protons,¹⁰ this energy can be estimated from nuclear physics as 16MeV/nucleon; therefore we can identify an *onset* value $\mu_o \simeq 922\text{MeV}$ at which point baryon density n_B jumps from zero to nuclear density $n_{B0} \simeq 0.16\text{fm}^{-3}$. Since the vacuum and nuclear matter coexist at this point, the value $\mu = \mu_o$ corresponds to the “room chemical potential” that would be measured should we ever be able to construct a suitable potentiometer! Because $n_B = -\frac{1}{V} \frac{\partial \Omega}{\partial \mu}$, the discontinuity implies a first order phase transition. We expect the transition to persist for $T \neq 0$ on grounds of continuity, and therefore show it as a coexistence line emerging from $\mu = \mu_o$ in Fig. 3. As it now separates a phase in which baryons can be present but are dilute from one in which they are condensed, it is known as the *nuclear liquid-vapour transition* [8, 25]. It is anticipated that the line ends at a critical point with $T_c \simeq O(10\text{MeV})$; it is possible that critical opalescence has been detected near this point in the form of the broad distribution of fragment sizes observed in medium-energy nuclear collisions [26].

What happens as μ , and hence n_B , increase? Unfortunately the lattice gauge theory simulations which were so useful along the T -axis become ineffective once applied to QCD with $\mu \neq 0$. For densities up to $2 - 3n_{B0}$ we can extrapolate from our current knowledge of nuclear physics [27]. Beyond that we are forced to rely on approximate treatments such as the bag model [8]. As n_B increases we again expect a transition from a phase in which matter exists in the form of nucleons to a higher entropy phase where the dominant degrees of freedom are quarks. Naively this should occur at densities of the order of a billion tonnes per teaspoonful where the volume per baryon equals the baryon volume, and the bag surfaces just touch. For degenerate

when the mean time between collisions is less than the natural lifetime.

¹⁰Electromagnetic interactions, of course, play a pivotal role in determining the size and stability of atomic nuclei, and are also important in modelling neutron star interiors. On the energy scales depicted in Fig. 3, however, it is reasonable to neglect them.

neutron matter at this critical density we have

$$n_{Bc} \simeq 2 \int_0^{k_F} \frac{4\pi k^2}{(2\pi)^3} dk = \frac{k_F^3}{3\pi^2} \simeq \frac{(\mu_c^2 - M^2)^{\frac{3}{2}}}{3\pi^2} \simeq \frac{1}{R^3} \simeq 1\text{fm}^{-3}, \quad (5.1)$$

giving $\mu_c \sim 1200\text{MeV}$. Various model estimates yield $\mu_c \sim 1100 - 1500\text{MeV}$, and the jump in density at the transition $\Delta n_B \sim 2 - 5n_{B0}$ [28, 29].

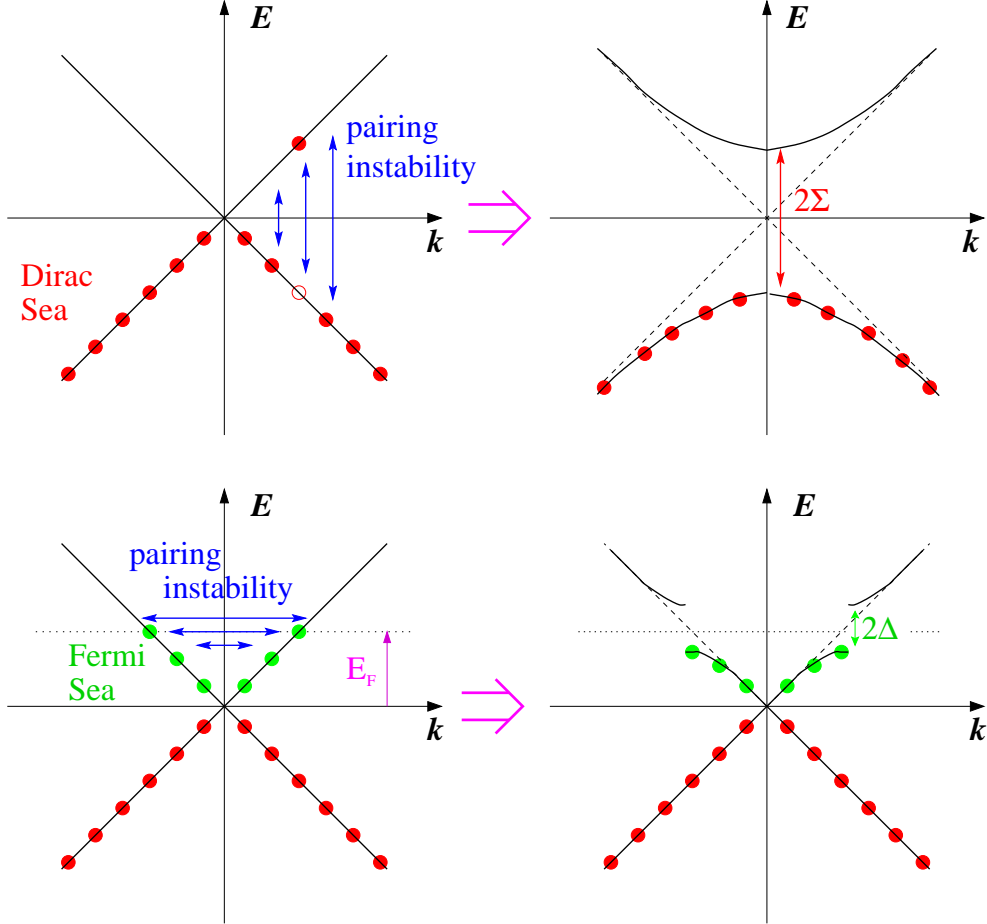


Figure 13: Pairing instabilities leading to chiral symmetry breaking (top), and superconductivity (bottom)

Let's discuss the nature of this *quark matter* (QM) phase. In the bag model, the QM phase corresponds to the bag interior in which chiral symmetry is restored and quarks are light. That this might be so on more general grounds is illustrated in the upper part of Fig. 13, where χSB is shown as due to a pairing instability between quarks and anti-quarks of equal and opposite momenta; the \bar{q} are here interpreted as

holes in the *Dirac Sea* of negative energy states. χ SB occurs if the binding energy of the $q\bar{q}$ pair exceeds the energy needed to excite them: the result is the modified single-particle excitation spectrum shown at upper right, with an energy gap 2Σ between the highest occupied and lowest empty states. Now when $n_B > 0$, some positive energy states are also occupied, as shown at bottom left; we refer to these as belonging to the *Fermi Sea*. It is impossible to excite $q\bar{q}$ pairs if the q state has momentum $k < k_F$ and is hence already in the Fermi Sea; such pairs are *Pauli-blocked*. At some point, therefore, available $q\bar{q}$ states require so much energy to excite that it is preferable to revert to a chirally symmetric ground state. Since $k_F \gtrsim \mu_c/3 \gg m_{u,d}$, we deduce the quarks near the Fermi surface which participate in QM's interaction with other forms of matter are highly relativistic.

Where might QM be found? If the sequence of phases outlined above is correct, then only at the onset $\mu = \mu_o$ does pressure $P = -\Omega/V$ vanish, implying that nuclear matter at this point is stable and self-bound. To reach the higher densities needed for QM an external pressure is needed; the most likely source is the gravitational binding in the compact astrophysical objects of mass $O(10^{30}\text{kg})$ and radius $O(10\text{km})$ known as *neutron stars* [27]. Neutron star central densities are estimated as lying in the range $5 - 10n_{B0}$. It turns out that the maximum mass a neutron star can have before becoming unstable with respect to further gravitational collapse to form a black hole depends on how compressible its material is, as determined by the equation of state:

$$PV^\Gamma = \text{constant}. \quad (5.2)$$

Roughly speaking [27], $\Gamma \simeq \frac{5}{3}$ for non-relativistic matter such as neutrons with $\mu \lesssim \mu_c$, producing a “stiff” equation of state and limiting masses $\gtrsim 2M_\odot$, where M_\odot is the mass of the sun; relativistic QM, on the other hand, has $\Gamma \simeq \frac{4}{3}$, implying a softer equation at the core, and hence a lower limiting mass. So far observed neutron star masses have not exceeded $1.4M_\odot$, which does not exclude models for their structure which include a QM core [30]. It may well turn out that our best experimental probe of QM will come through careful observation of the known neutron star population, currently $\sim 10^3$, focussing on quantities such as the rate of change of angular momentum, cooling rate, and magnetic field. One interesting possibility is that once $\mu/3 \gtrsim m_s$ the ground state of matter includes an appreciable fraction of strange quarks, and hence a composition $\sim uds$; neutron stars may actually be made of such *strange quark matter* (SQM) [31]. It is even conceivable, though unlikely, that SQM

is the ground state for $P = 0$, and nuclear matter therefore only metastable.¹¹

Much recent interest has been aroused by the idea that QM might have richer properties than those of a simple relativistic fermi liquid. Consider the lower panel of Fig. 13: if the qq interaction is even weakly attractive at the Fermi surface, then another pairing instability, the so-called *BCS instability*, is expected between quark pairs at antipodal points, leading to a ground state with a non-vanishing *diquark condensate* $\langle qq \rangle \neq 0$ [32, 33, 34]. Analogously to χ SB, the instability leads to an energy gap 2Δ between highest occupied and lowest vacant one-particle states, the distinction being that this time the gap is located at the Fermi surface. In metals at temperatures of a few kelvin, a BCS instability can arise between *Cooper pairs* of electrons due to an attractive force arising from interaction with vibrations of the underlying crystal lattice of positively-charged ions. The Cooper pair condensate leads to the phenomenon of *superconductivity*, signalled by electric current flowing without resistance in a narrow layer close to the sample surface; the screening effect of this supercurrent results in the *Meissner effect*, namely the complete exclusion of magnetic field from the sample. A BCS instability between neutral helium atoms in liquid ^3He at milli-kelvin temperatures, on the other hand, leads to frictionless flow and quantisation of vorticity, a phenomenon known as *superfluidity*.

In QCD the force between two quarks due to single gluon exchange is attractive (unlike single photon exchange between two electrons), implying that a weak BCS instability should be present in QM [32]. More recent calculations which attempt to model realistic strong interactions in the regime $\mu \gtrsim \mu_c$ predict a much bigger effect, with Δ as large as 10 - 100MeV [35]. What physical consequences might arise? A crucial consideration, not applicable to χ SB, is that the qq wavefunction is constrained by the Pauli Exclusion Principle. As a result the ground state is sensitive to the flavor composition of the available quarks. Suppose $\mu/3$ is not much greater than m_s ; in this case $k_{Fs} \ll k_{Fu,d}$ and pairing is effectively restricted to the two light flavors. The diquark condensate which thus forms is [33, 34]

$$\langle qq \rangle_{2SC} = \epsilon^{\alpha\beta 3} \epsilon_{ab} \langle \psi_a^\alpha(k, \uparrow) \psi_b^\beta(-k, \downarrow) \rangle \neq 0. \quad (5.3)$$

The quark spins are combined in an antisymmetric singlet state; the overall antisymmetry of (5.3) under quark exchange is then enforced by the alternating ϵ tensors acting on flavor $a, b = 1, 2$ and color $\alpha, \beta = 1, \dots, 3$ indices. Now, since the qq_{2SC}

¹¹It has been suggested that catastrophic consequences might follow if SQM were produced at rest in a heavy-ion collision at RHIC; the resulting “strangelet” might seed the conversion of the entire Earth to SQM via weak interactions! Fortunately (at time of writing) this has not yet come about.

wavefunction is not color-neutral, we infer by analogy with the electrically-charged Cooper pair that the ground state is *color superconducting*. The most immediate consequence is that out of the eight gluons, the five which carry color #3 acquire a mass of $O(\Delta)$ and hence cannot penetrate QM over distances much greater than a screening length $\sim \Delta^{-1}$, in direct analogy with the Meissner effect in metallic superconductors.¹² The three gluons left massless carry combinations of only the first two colors. The qq_{2SC} wavefunction however, like the QGP, respects chiral symmetry; for this reason although the superconducting description will be the more natural for $T \lesssim \Delta$, there may well be no true transition separating 2SC and QGP phases, and we have shown them separated by a crossover in Fig. 3.

For larger μ , k_{Fs} should increase up to the point where strange quarks can participate in the pairing. In this case a more symmetric “color-flavor-locked” (CFL) condensate can form:

$$\langle qq \rangle_{CFL} = \sum_i \epsilon^{\alpha\beta i} \epsilon_{abi} \langle \psi_a^\alpha(k, \uparrow) \psi_b^\beta(-k, \downarrow) \rangle \neq 0. \quad (5.4)$$

If anything the CFL state is still more exotic [33]; all 8 gluons are rendered massive implying color superconductivity, and chiral symmetry is also broken. Moreover, since the qq_{CFL} operator either creates or annihilates two units of baryon number, B is no longer a good quantum number – it can be shown that this B -violation leads to superfluidity. The CFL state is currently believed to be the stable ground state of matter as $\mu \rightarrow \infty$, and is shown as a distinct phase in Fig. 3.

Observational and experimental evidence for these fascinating new phases may be difficult to acquire. Since neutron star temperatures are typically $\lesssim 10\text{MeV}$, it may seem that they are a natural place to look. However, two factors work against us; even if a neutron star has a QM core its bulk is probably normal nuclear matter, and color superconductivity is a phenomenon confined to the vicinity of the Fermi surface rather than the whole Fermi Sea and therefore has relatively little impact on the equation of state. Both imply that any effect of color superconductivity is likely to be quite subtle. One prediction is that a color superconducting core would stabilise neutron star magnetic fields and prevent them from decaying over cosmologically significant timescales [36]. Another speculation concerns the formation of a neutron star by core collapse of a very massive star during a supernova explosion [37]. During this violent

¹²In weak interaction physics the identical effect, now known as the *Higgs phenomenon*, arises as a consequence of the condensation of a scalar *Higgs field* and gives W^\pm and Z^0 bosons masses of $O(100\text{GeV})$, restricting the effective range of the weak interaction to 10^{-18}m .

event the star cools from $\sim 50\text{MeV}$ to $\sim 10\text{MeV}$ over a timescale of a few seconds by emission of massless weakly-interacting particles called *neutrinos* ν , $\bar{\nu}$.¹³ If a transition to superconducting QM occurs in this period, ν - q scattering with $k \lesssim \Delta$ will be Pauli-blocked, with the effect of making the core effectively transparent to neutrinos. They may emerge from the collapsing core in a sudden burst, rather than steadily diffusing out over 10-20 seconds as in standard collapse scenarios; it may be feasible to detect such a burst in terrestrial neutrino detectors.

6 Conclusion

In this article I have explained how the study of the strong interaction has spawned a new field, QCD thermodynamics, and argued that the resulting phase diagram may be surprisingly rich. An interesting feature for both $T > 0$, $\mu > 0$ has been the important role played by the strange quark; the fine details of Fig. 3 may be very sensitive to the precise value of m_s . One aspect we should return to is the possibility of a second critical point in the (T, μ) plane, whose existence follows if we assume that the thermal transition is continuous or a crossover, whereas the density transition is first order [28]. Its location is hard to calculate using present technology (one estimate is $\sim (0.8T_c, 0.6\mu_c)$ [29]), but is expected to move to the left as m_s decreases; recall that for 3 light quarks it should merge with the T -axis to produce a first-order thermal transition. It has been proposed that various critical phenomena in the vicinity of this point could be detected in RHIC collisions [38]. The reason that the strange quark has such a big influence on QCD thermodynamics is that m_s is of the same order of magnitude as the “interesting” QCD scale $200\text{MeV} \simeq 1\text{fm}^{-1}$ which has cropped up repeatedly in our discussion. This scale characterises all QCD phenomena not described by single gluon exchange; there is a sense in which it is the scale at which the strong interaction becomes “strong”.

Apart from the obvious attraction of exploring new states of matter, why is it important to continue study in this direction? Firstly, QCD is an exceedingly challenging theory, and the experiments and observations I have sketched provide a new arena in which to test its predictions. It is gratifying how far we can get via fairly simple thermodynamic arguments, coupled with insights from relativity and quantum theory. However, it is also a particularly satisfying area to work in for theorists using

¹³An anti-neutrino is produced in the archetypal weak interaction, β -decay of the neutron, via $d \rightarrow ue^- \bar{\nu}$.

systematic calculational techniques such as lattice gauge theory, since by and large their theoretical predictions still pre-date (and hence inform) experiment, rather than lag behind by, in certain cases, several tens of years. Secondly, QCD thermodynamics deals with the only phase transition in particle physics which will ever be studied under laboratory conditions. Phase transitions in other particle physics contexts, such as electroweak or grand unified theories, are believed to have played a crucial role in the first instants of the universe following the Big Bang; they have been invoked in mechanisms to account for the large-scale structure of the universe as revealed by the distribution of galaxy clusters, the observed excess of matter over anti-matter, and also the period of early exponentially rapid expansion invoked to account for the observed homogeneity of the cosmic microwave background. A quantitative understanding of both equilibrium and non-equilibrium thermodynamics in these models will be required before the full story can be told; QCD offers our sole opportunity of thoroughly testing that understanding.

Acknowledgements

It is my pleasure to thank the Bielefeld lattice group led by Frithjof Karsch, the Birmingham ALICE group, and the authors of [33], not simply for their help with preparing some of the figures, but also for introducing me to the complexities and excitement of this subject.

References

- [1] M. Gell-Mann, Phys. Lett. **8** (1964) 214;
G. Zweig, CERN reports TH-402, TH-412 (1964).
- [2] R.P. Feynman, Phys. Rev. Lett. **23** (1969) 1415;
J.D. Bjorken, Phys. Rev. **179** (1969) 1547.
- [3] A very good introduction to the lattice method is J.B. Kogut, Rev. Mod. Phys. **55** (1983) 775. See also M. Creutz, *Quarks, Gluons and Lattices*, (Cambridge University Press, 1983), and I. Montvay and G. Münster, *Quantum Fields on a Lattice*, (Cambridge University Press, 1994).
- [4] D.J. Gross and F. Wilczek, Phys. Rev. Lett. **30** (1973) 1343;
H.D. Politzer, Phys. Rev. Lett. **30** (1973) 1346.

- [5] P. Pennanen, A.M. Green and C. Michael, Phys. Rev. **D56** (1997) 3903.
- [6] A. Chodos, R.L. Jaffe, K. Johnson, C.B. Thorn and V.F. Weisskopf, Phys. Rev. **D9** (1974) 3471.
- [7] A. Casher, Phys. Lett. **B83** (1979) 395.
- [8] see, eg. J.I. Kapusta, *Finite-Temperature Field Theory*, (Cambridge University Press, 1989).
- [9] F. Karsch, E. Laermann and A. Peikert, Phys. Lett. **B478** (2000) 447; Bielefeld report BI-TP2000/41 hep-lat/0012023, and F. Karsch, private communication.
- [10] K. Kajantie, M. Laine, J. Peisa, A. Rajantie, K. Rummukainen and M. Shaposhnikov, Phys. Rev. Lett. **79** (1997) 3130.
- [11] R.V. Gavai, J. Potvin and S. Sanielevici, Phys. Rev. Lett. **58** (1987) 2519; E. Laermann, Nucl. Phys. **B**(Proc. Suppl.) **63** (1998) 114.
- [12] R.N. Boyd and T. Kajino, Ap. J. **336** (1989) L55; R.A. Maloney and W.A. Fowler, Ap.J. **345** (1989) L5.
- [13] A good introduction is C.-Y. Wong, *Introduction to High-Energy Heavy-Ion Collisions*, (World Scientific, Singapore, 1994). A recent review of the experimental situation at the SPS is U. Heinz, Nucl. Phys. **A685** (2001) 414. Also see <http://cern.web.cern.ch/CERN/Announcements/2000/NewStateMatter>.
- [14] NA49 Collaboration, H. Appelshäuser *et al*, Phys. Rev. Lett. **82** (1999) 2471.
- [15] J.D. Bjorken, Phys. Rev. **D27** (1983) 140.
- [16] NA49 Collaboration, T. Alber *et al*, Phys. Rev. Lett. **75** (1995) 3814; WA98 Collaboration, M. Aggarwal *et al*, Nucl. Phys. **A610** (1996) 200c.
- [17] R. Hanbury-Brown and R.Q. Twiss, Nature **127** (1956) 27.
- [18] B. Tomášik, U.A. Wiedemann and U. Heinz, CERN report TH-215 (1999), nucl-th/9907096.
- [19] T. Matsui and H. Satz, Phys. Lett. **B178** (1986) 416; H. Satz, Rep. Prog. Phys. **63** (2000) 1511.

- [20] E. Eichten, K. Gottfried, T. Kinoshita, K.D. Lane and T.M. Yan, Phys. Rev. **D21** (1980) 203.
- [21] NA50 Collaboration, M. Abreu *et al*, Phys. Lett. **B477** (2000) 28.
- [22] WA97 Collaboration, E. Andersen *et al*, Phys. Lett. **B433** (1998) 209.
- [23] J. Rafelski and B. Müller, Phys. Rev. Lett. **48** (1982) 1066;
P. Koch, B. Müller and J. Rafelski, Phys. Rep. **142** (1986) 167.
- [24] CERES Collaboration, B. Lenkeit *et al*, Nucl. Phys. **A661** (1999) 23c.
- [25] L.P. Csernai and J.I. Kapusta, Phys. Rep. **131** (1986) 223.
- [26] W. Trautmann, proceedings of *International Summer School On Correlations And Clustering Phenomena In Subatomic Physics* (Dronten 1996) p. 115, nucl-ex/9611002.
- [27] see, eg. S.L. Shapiro and S.A. Teukolsky, *Black Holes, White Dwarfs and Neutron Stars*, (Wiley, 1983).
- [28] S.P. Klevansky, Rev. Mod. Phys. **64** (1992) 649.
- [29] M.A. Halasz, A.D. Jackson, R.E. Shrock, M.A. Stephanov and J.J.M. Verbaarschot, Phys. Rev. **D58**:096007 (1998).
- [30] A recent review is H. Heiselberg and M. Hjorth-Jensen, Phys. Rep. **328** (2000) 237.
- [31] E. Witten, Phys. Rev. **D30** (1984) 272;
E. Fahri and R.L. Jaffe, Phys. Rev. **D30** (1984) 2397.
- [32] D. Bailin and A. Love, Phys. Rep. **107** (1984) 325.
- [33] M. Alford, K. Rajagopal and F. Wilczek, Phys. Lett. **B422** (1998) 247; Nucl. Phys. **B537** (1999) 443.
- [34] R. Rapp, T. Schäfer, E.V. Shuryak and M. Velkovsky, Phys. Rev. Lett. **81** (1998) 53.
- [35] J. Berges and K. Rajagopal, Nucl. Phys. **B538** (1999) 215.

- [36] M. Alford, J. Berges and K. Rajagopal, Nucl. Phys. **B571** (2000) 269.
- [37] G.W. Carter and S. Reddy, Phys. Rev. **D62**:103002 (2000).
- [38] M.A. Stephanov, K. Rajagopal and E.V. Shuryak, Phys. Rev. Lett. **81** (1998) 4816.

About the Author

Simon Hands obtained a Ph.D. in theoretical particle physics from the University of Edinburgh in 1986, and has subsequently held research posts at the Universities of Oxford, Illinois and Glasgow, and in the Theory Division at CERN. In 1992 he won a bottle of vintage champagne from the then Minister of Science, William Waldegrave, for one of the five best responses to his challenge to describe the Higgs boson on one A4 sheet! In 1993 he joined the newly-formed theory group at the University of Wales Swansea as a PPARC Advanced Research Fellow, and is now Reader in Physics. Dr. Hands' research has centred on using lattice gauge theory techniques to study dynamical symmetry breaking in strongly-interacting quantum field theories like QCD, most recently specialising to the case of non-zero μ and T . Currently he enjoys the use of a special-purpose multi-processor APEMille computer at Swansea, capable of over 20 billion complex arithmetic operations per second, but more power is always welcomed.

email: `s.hands@swansea.ac.uk`